7th International Building Physics Conference

IBPC2018

Proceedings

SYRACUSE, NY, USA

September 23 - 26, 2018

Healthy, Intelligent and Resilient
Buildings and Urban Environments

ibpc2018.org | #ibpc2018

Unsteady-state exergy analysis on two types of building envelopes under time-varying boundary condition

Wonjun Choi[1,*], Ryozo Ooka[1] and Masanori Shukuya[2]

[1]Institute of Industrial Science, The University of Tokyo
[2]Department of Restoration Ecology and Built Environment, Tokyo City University

[*]*Corresponding email: wonjun@iis.u-tokyo.ac.jp*

ABSTRACT
In the built environment, the thermal exergy behavior is very sensitive to the change of environmental temperature, because the temperature difference between the reservoir and a system of interest is small. Moreover, the transient characteristics become very important for the building envelope, which is primarily affected by the environmental temperature changes and has a relatively large heat capacity. Most of the exergy analyses have been performed under steady-state assumption. However, it may miss some important details of the transient process. Thus, when the transient transfer process becomes important, the unsteady-state exergy analysis should be conducted. In this study, we propose complete energy, entropy, and exergy equations in their partial differential forms. By solving them numerically, we examined the transient exergy process inside the building envelope composed of concrete and insulation layers under time-varying boundary condition. Using this new methodology, we can improve the temporal and spatial resolution of the exergy analysis and thus provide more complete information about exergetic behavior.

KEYWORDS
Unsteady-state heat conduction; Thermodynamics; Numerical exergy analysis; Warm and cool exergy; Building envelope

INTRODUCTION
Applying exergy analysis method to a system of interest, we can quantify the part of the energy supplied that is not converted into work and the one that is converted (Shukuya, 2013). Here, we want to focus more on the temporal change of system state and discuss it in more detail. This transient exergetic process has not been well understood yet, because the majority of the exergy analyses have been conducted under steady-state assumption.

Consider building envelope as the system of interest, which is primarily affected by the dynamic change of the environmental temperature. In general, the building envelope has low thermal conductivity and large thermal capacity. Thus, when there is a temperature difference between the boundaries, the temperature distribution inside the envelope is not uniform. With respect to the environmental temperature, a very complex exergy process occurs that is dependent on the outer and inner surface temperatures, temperature distribution inside the envelope, and indoor air temperature. In other words, if we consider the building envelope as several discretized subsystems, the direction of heat flow changes dynamically with time due to the relationship between the temperatures of the adjacent subsystems. Consequently, the state and flow of warm or cool exergy and consumption change dynamically as well. For such a system, applying steady-state assumption could overlook some important details of the transient processes. Thus, when the transient exergy transfer process becomes important, an unsteady-state exergy analysis should be conducted.

Recently, we have proposed a complete form of unsteady-state exergy analysis which can be applied to any heat conduction problem (Choi, Ooka, & Shukuya, 2018). The governing equations for the energy, entropy, and exergy were presented in the differential form. Moreover, the numerical solution approach was described in detail and the numerical integrity of proposed methodology was verified by comparing the numerical result with the steady-state analytical solution. In this study, based on the developed method for unsteady-state exergy analysis, we studied transient exergy process in building envelopes.

GOVERNING EQUATIONS FOR UNSTEADY-STATE EXERGY ANALYSIS

Partial differential forms for energy, entropy and exergy equations

The governing equations for one-dimensional energy, entropy, and exergy transfers are given by Eqs. (1), (2), and (3), respectively. The details can be found in (Choi et al., 2018).

$$\frac{\partial Q}{\partial t} = -\frac{\partial q}{\partial x} \tag{1}$$

$$\frac{\partial S_{st}}{\partial t} = -\frac{\partial}{\partial x}\left(\frac{q}{T}\right) + q\frac{\partial}{\partial x}\left(\frac{1}{T}\right) \tag{2}$$

$$\frac{\partial X_{st}}{\partial t} = -\frac{\partial}{\partial x}\left(q - T_0\frac{q}{T}\right) - q\frac{\partial}{\partial x}\left(\frac{1}{T}\right)T_0 \tag{3}$$

Here, the infinitesimal change of thermal energy stored in a unit volume and the rate of heat flux are defined as $\partial Q = C\partial T$ and $q = -k(\partial T/\partial x)$, respectively. Additionally, $\partial S_{st}(= \partial Q/T)$ is the stored entropy, $X_{st}(= Q - T_0 S_{st})$ is the stored exergy, C is the volumetric thermal capacity, T is temperature, t is time, x is the space coordinate, k is the thermal conductivity and T_0 is the environmental temperature. It should be noted that the temperature used in the entropy and exergy equations is the absolute temperature and has the units of Kelvin.

Discretized form of energy, entropy, and exergy equations

Using finite difference method, the governing equations can be solved. We used a central difference scheme and the hybrid Crank-Nicolson scheme for the temporal and spatial discretization, respectively. The discretized forms of the energy, entropy, and exergy equations are given by Eqs. (4), (5), and (6), respectively. The entropy and exergy equations are written in the form of [inflow] - [entropy generation or exergy consumption] = [stored] + [outflow] to explicitly represent the balance within the system.

$$\frac{T_i^{n+1} - T_i^n}{\Delta t} = \frac{1}{2C_i\Delta x_i}\left\{-q_{i_+}^n + q_{i_-}^n - q_{i_+}^{n+1} + q_{i_-}^{n+1}\right\} \tag{4}$$

$$\sigma_{fi,i} + \sigma_{g,i} = \sigma_{st,i} + \sigma_{fo,i} \tag{5}$$

$$\chi_{fi,i} - \chi_{c,i} = \chi_{st,i} + \chi_{fo,i} \tag{6}$$

It should be noted that each term in Eqs. (2) and (3) has the units of W/(m^3·K) and W/m^3, respectively, but Eqs. (5) and (6) have the units of W/(m^2·K) and W/m^2, respectively. Each term in Eqs. (5) and (6) has the following forms: entropy inflow, $\sigma_{fi,i} = \left(q_{i\_}/T_{i\_}\right)\Big|^{n+0.5}$, entropy generation, $\sigma_{g,i} = (\Delta x_i/k_i)\left(q_i^2/T_i^2\right)\Big|^{n+0.5}$, entropy stored, $\sigma_{st,i} = \Delta x_i C_i\left(T_i^{n+1} - T_i^n\right)/\Delta t(T_i)|^{n+0.5}$,

entropy outflow, $\sigma_{fo,i} = \left(q_{i_+}/T_{i_+}\right)\big|^{n+0.5}$, exergy inflow, $\chi_{fi,i} = \left\{q_{i_-}\left(1 - T_0/T_{i_-}\right)\right\}\big|^{n+0.5}$, exergy consumption, $\chi_{c,i} = (\Delta x_i/k_i)\left(q_i{}^2\, T_0/T_i^2\right)\big|^{n+0.5}$, exergy stored, $\chi_{st,i} = \Delta x_i C_i(1 - T_0/(T_i)|^{n+0.5})\left(\left(T_i^{n+1} - T_i^n\right)/\Delta t\right)$, and exergy outflow, $\chi_{fo,i} = \left\{q_{i_+}\left(1 - T_0/T_{i_+}\right)\right\}\big|^{n+0.5}$. Additionally, the subscript i is the i-th node, i_+ and i_- are the quantities defined between the nodes i and $i+1$, and $i-1$ and i, respectively, superscript n is the time step and $n+0.5$ is the time step required for the Crank-Nicolson scheme. The detailed definition of each quantity and numerical scheme used can be found in (Choi et al., 2018).

PROBLEM SETTING

Concrete and insulation layers which have a thickness of 10 cm and 6 cm, respectively, were considered. Its thermal properties are listed in Table 1. To examine the difference in exergetic behavior depending on the location of insulation, two different envelope configurations were used. From the outside, the wall composition in the order of insulation–concrete or concrete–insulation is referred to as IC or CI, respectively (Figure 1).

The envelope was discretized at the uniform intervals of 1 cm as shown in Figure 1. The calculation conditions are summarized in Table 2. The total calculation period was 180 h, but the first 120 h were considered as the warm-up period. Thus, we only present the results of the last 60 h. Time-varying Dirichlet boundary condition (BC) using 24-h period sine curve was assigned for the outer surface BC, T_{os} and regarded as the environmental temperature, T_0. For the inner surface BC, T_{is}, the constant temperature of 20 °C was assigned.

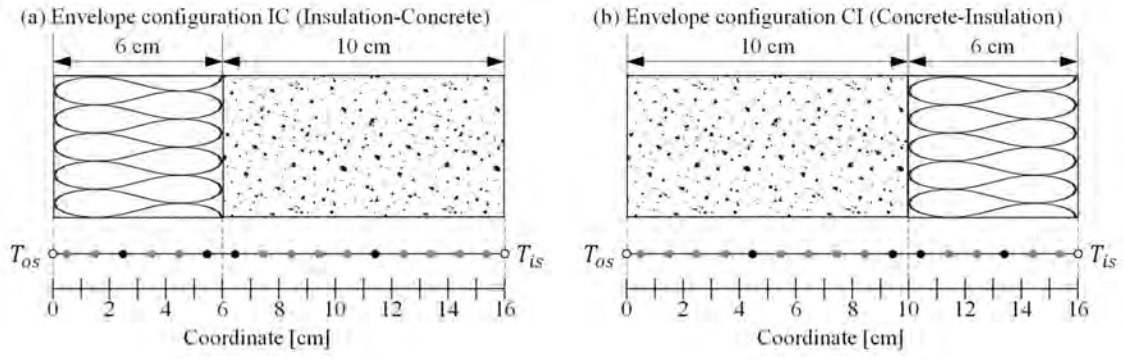

Figure 1. Schematic of two envelope configurations and nodes (T_{os}: outer surface boundary temperature, T_{is}: inner surface boundary temperature).

Table 1. Thermal properties of concrete and insulation.

Material	Thermal conductivity	Specific thermal capacity	Density
Concrete	1.5 W/(m·K)	2000 J/(kg·K)	1000 kg/m^3
Insulation	0.04 W/(m·K)	1500 J/(kg·K)	30 kg/m^3

Table 2. Calculation conditions (T_{ini}: initial temperature of calculation domain).

Time step	Calculation period	T_{ini} [°C]	$T_{os} = T_0$ [°C]	T_{is} [°C]
20 s	180 h (120 h warm up)	20	$T_{os} = 20 + 10\sin\left(\frac{2\pi t}{24 \cdot 3600}\right)$	20

RESULTS

Energy results

The temperature variations obtained by solving the energy equation are shown in Figure 2 (a) and (b). In IC, the effect of time-varying outer BC reduces significantly through the insulation layer. As a result, the temperature near the interface between two material layers (near x = 6 cm) does not change a lot from the inner BC of 20 °C, and consequently the change of the external BC does not have a significant influence on the concrete layer. On contrary, CI has the concrete layer with low thermal resistance of the outer side, and thus the effect of time-varying T_{os} is transmitted through the concrete layer to the outer surface of the insulation layer without significant attenuation. Therefore, the interface temperature (near x = 10 cm) in CI is affected more by the change of T_{os} compared to that in IC.

In the plots of heat flux (Figure 2 (c) and (d)), we can observe a large difference between two cases. It should be noted that the direction of q from the outer to inner surface is defined as the positive value. The maximum magnitude of q in IC occurs at the outermost surface (approximately ±6.5 W/m^2) and there is no significant difference between the insulation and concrete layers (Figure 2 (c)). In contrast, in CI, the difference in q between the layers is significant. In concrete layer, the maximum q of ~±130 W/m^2 is generated at the outermost surface, but the one in the insulation layer is ~±6 W/m^2 only, that is almost of the same magnitude as the maximum q in IC (Figure 2 (d)).

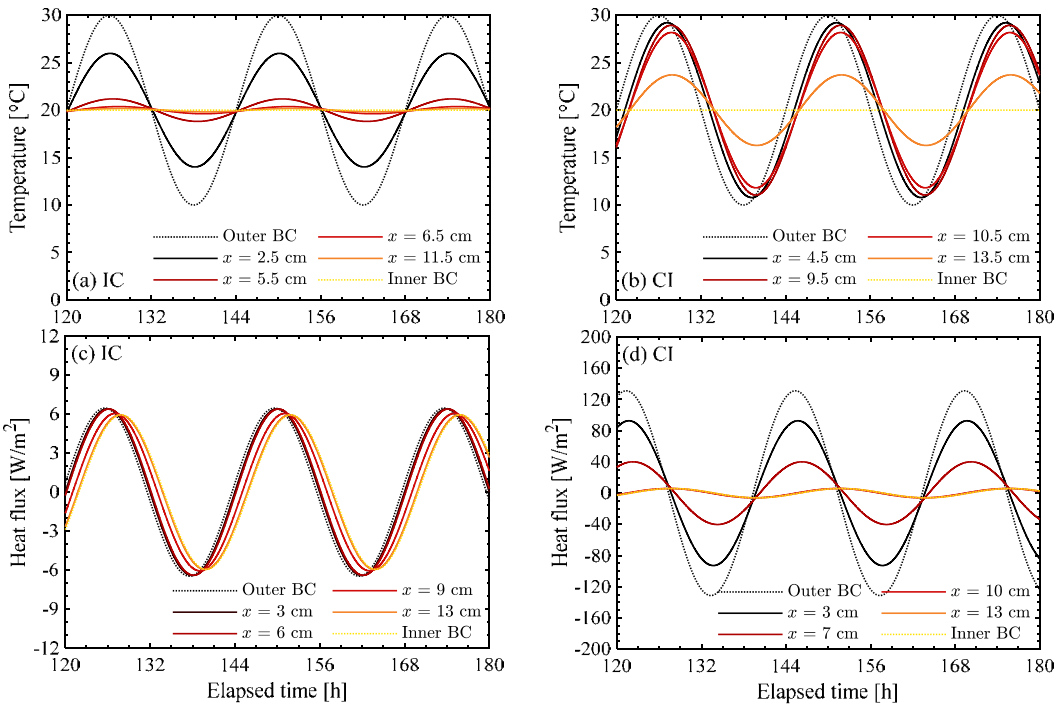

Figure 2. Node temperatures and heat flux at the interfaces: (a) temperature in IC; (b) temperature in CI; (c) heat flux in IC; and (d) heat flux in CI

Exergy results

Based on the results for the temperature and heat flux, entropy and exergy calculations are performed. Because the entropy is considered in the exergy equation, only the results of the exergy are presented. Figure 3 shows the exergy consumption rate, χ_c, stored rate, χ_{st}, and flow, χ_f, for some nodes and at the interfaces in the computational domain. The dashed and solid lines represent the values in insulation and concrete layers, respectively.

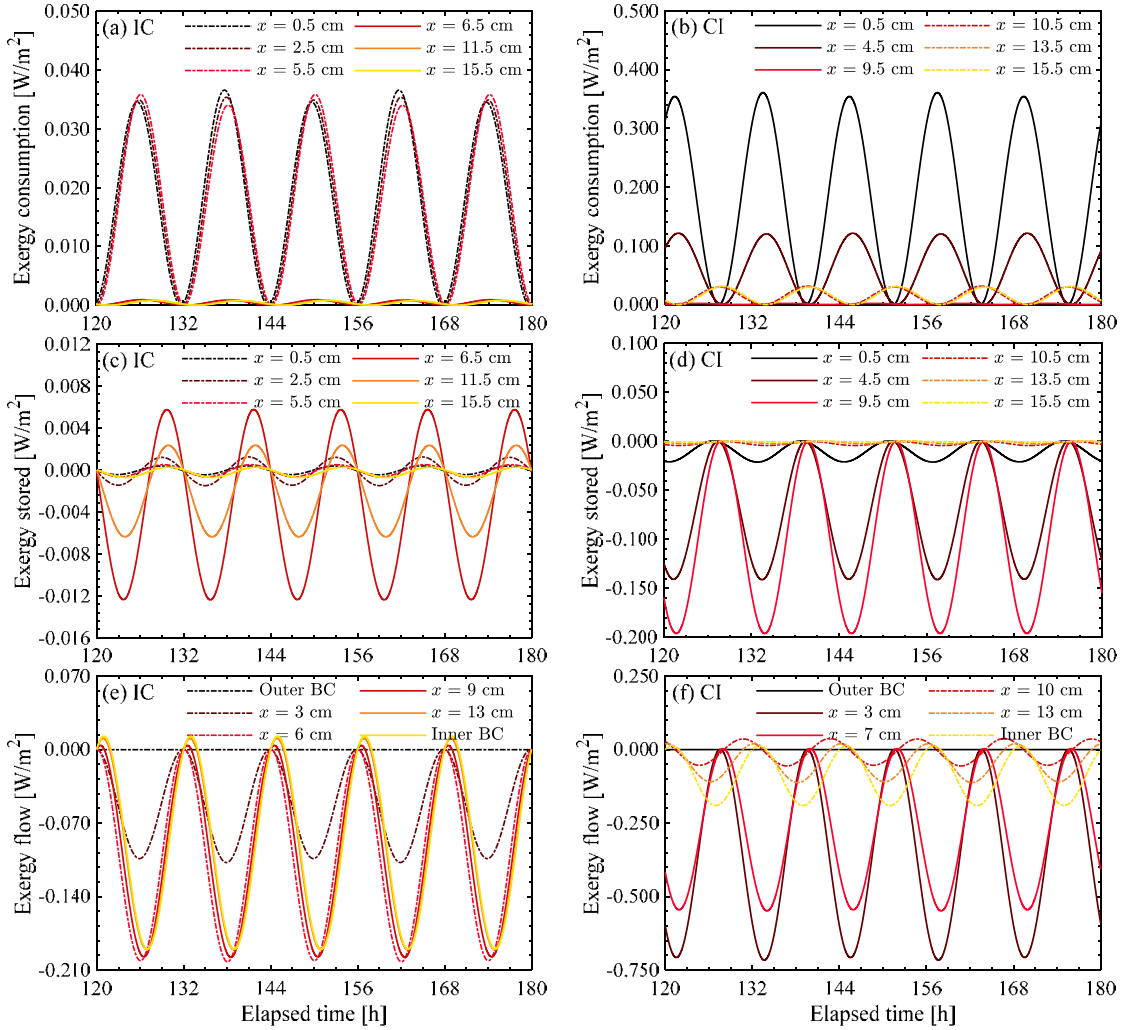

Figure 3. Exergy consumption rate, exergy stored rate, and exergy flow: (a) exergy consumption in IC; (b) exergy consumption in CI; (c) exergy stored in IC; (d) exergy stored in CI; (e) exergy flow in IC; and (f) exergy flow in CI.

Figure 3 (a) and (b) show that the maximum χ_c in CI is 10 times larger than that in IC (Note the difference in scales of vertical axes). This is because the heat flux, q, presented in Figure 2 is the dominant factor influencing χ_c. If the magnitude of q is similar, the larger the resistance, the greater the exergy consumption. It can be confirmed when we compare the magnitudes of χ_c in the insulation and concrete layers of IC.

The exergy stored rate, χ_{st}, is determined by Carnot coefficient $(1 - T_0/T_i)$ at the node, the time derivative of the node temperature $\partial T_i/\partial t$, and the volumetric heat capacity, C_i. Whether it becomes cool or warm is dependent on the sign of the node Carnot coefficient, and the increase or decrease of exergy stored rate is determined by the sign of χ_{st}. Because C_i of concrete is ~44 times larger than that of insulations (Table 2), we can observe large χ_{st} in the concrete layer for both cases (Figure 3 (c) and (d)). In addition, in terms of the time derivative of temperature, $\partial T_i/\partial t$ of the concrete layer in CI is larger than that in IC, because the effect of time-varying T_{os} is significantly reduced by the insulation layer placed at the outer side. Therefore, we can observe a large difference in χ_{st} for the concrete layer for IC and CI cases. Moreover, the behavior of χ_{st} changes depending on the location of the insulation. CI has

negative χ_{st} value for most times, which means that it moves only in a decreasing direction, whereas IC has a certain range of positive χ_{st} values.

The exergy flow, χ_f, is determined by the product of Carnot coefficient and heat flux. Because of the nature of the problem, that assumes the outer surface boundary as the environmental temperature, T_0, the exergy inflow at the outer surface is zero, because the Carnot coefficient is always zero at the outer surface (Figure 3 (e) and (f)). As shown in Figure 2 (c), IC has very small spatial variations in the magnitude of q. Thus, there is no significant spatial variations in χ_f (Figure 3 (e)). However, in CI, a large attenuation of q from the outer to inner surface is observed (Figure 2 (d)) and it leads to the large spatial variations of χ_f (Figure 3 (f)). As mentioned previously, the heat flux from the outer to inner surface was defined to be positive. Thus, if the exergy flow has a negative value with the associated heat flux to be positive, then it is a cool exergy flow and its direction is opposite to the heat flux (i.e., the flow is from the cell interface to the outer surface).

We further analyzed the effects of insulation location on χ_c for the entire envelope. The total χ_c for two configurations and χ_c in each material layer are shown in Figure 4 (a) and (b), respectively. In the insulation layer, χ_c in IC is slightly larger than that of CI. In contrast, in the concrete layer, there is a significant difference in χ_c between two cases. The maximum χ_c in concrete layer are ~0.008 W/m^2 and ~1.33 W/m^2 for IC and CI, respectively. This significant difference is because χ_c increases quadratically with the heat flux q_i^2. Therefore, the difference in q is further amplified in the results of χ_c. As a result, the total χ_c for the period of 120–180 h (i.e., $\chi_c \Delta t$) for IC and CI is 11.8 and 76.4 kJ/m^2, respectively.

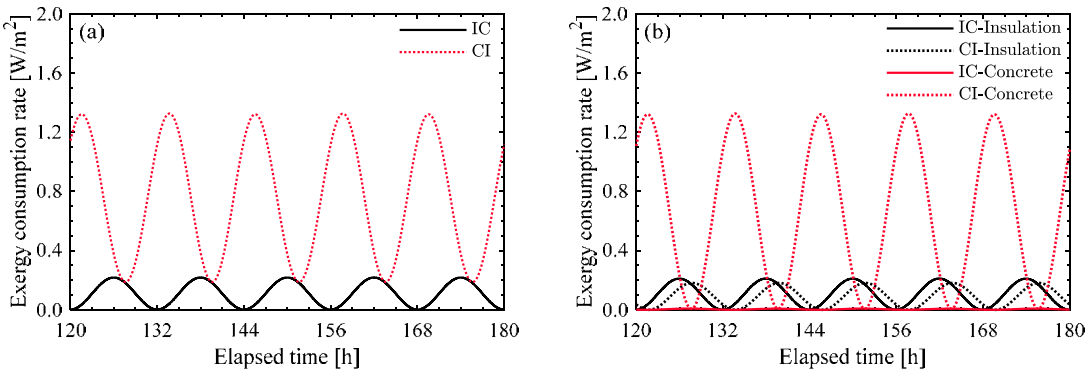

Figure 4. (a) total exergy consumption rate for two cases and (b) exergy consumption rate in insulation and concrete layers.

CONCLUSIONS

In this study, we have conducted an unsteady-state exergy analysis for two different building envelopes under time-varying boundary condition. This methodology provides insight into the transient exergetic behavior that is missing in the steady-state analysis. Moreover, it can provide higher temporal and spatial resolutions for the system of interest. In future, the studies will be conducted with more realistic problem setting considering radiative and convective exergy transfers.

REFERENCES

Choi, W., Ooka, R., & Shukuya, M. (2018). Exergy analysis for unsteady-state heat conduction. *International Journal of Heat and Mass Transfer*, 116, 1124–1142.

Shukuya, M. (2013). *Exergy: Theory and Applications in the Built Environment*. Springer.